

# The dual HDAC and PI3K inhibitor, CUDC-907, inhibits tumor growth and stem-like properties by suppressing PTX3 in neuroblastoma

MENGZHEN LI<sup>1,2\*</sup>, YANG HU<sup>1,2\*</sup>, JUAN WANG<sup>1,2\*</sup>, YANJIE XU<sup>1,2</sup>, YE HONG<sup>1,2</sup>, LI ZHANG<sup>1,2</sup>, QIUYUN LUO<sup>2</sup>, ZIJUN ZHEN<sup>1,2</sup>, SUYING LU<sup>1,2</sup>, JUNTING HUANG<sup>1,2</sup>, JIA ZHU<sup>1,2</sup>, YIZHUO ZHANG<sup>1,2</sup>, YI QUE<sup>1,2\*</sup> and FEIFEI SUN<sup>1,2\*</sup>

<sup>1</sup>Department of Pediatric Oncology, Sun Yat-sen University Cancer Center; <sup>2</sup>State Key Laboratory of Oncology in South China, Guangdong Provincial Clinical Research Center for Cancer, Collaborative Innovation Center for Cancer Medicine, Sun Yat-sen University Cancer Center, Guangzhou, Guangdong 510060, P.R. China

Received July 26, 2023; Accepted November 1, 2023

DOI: 10.3892/ijo.2023.5602

**Abstract.** Neuroblastoma (NB) is one of the common solid tumors in childhood and poses a threat to the lives of children. Patients with advanced-stage or recurrent NB have a poor prognosis. CUDC-907, as a novel dual-target inhibitor of histone deacetylase (HDAC) and phosphatidylinositol-3-kinase (PI3K), has been proven to play an antitumor role in several types of tumors. However, the exact role of CUDC-907 in NB remains unclear. In the present study, *in vivo* and *in vitro* assays were performed to investigate the anti-NB activity of CUDC-907. Pentraxin 3 (PTX3) small interfering RNA (siRNA) and PTX3 overexpression plasmid were transfected into cells to define the underlying mechanisms of CUDC-907. Tumor tissues and clinical information were collected and immunohistochemistry (IHC) was conducted to analyze the association between the expression of HDAC1, HDAC2, HDAC3 and CD44, and the prognosis of patients with NB. The results indicated that CUDC-907 significantly inhibited the proliferation and migration, and induced the apoptosis of NB cells, downregulating the expression level of MYCN, and suppressing the PI3K/AKT and MAPK/ERK pathways. Furthermore, CUDC-907 suppressed the stem-like properties of NB cells by inhibiting PTX3, a ligand and upstream protein of CD44. IHC revealed that the high expression of HDAC1, 2,

3 and CD44 was associated with a poor prognosis of patients with NB. On the whole, these findings indicate that CUDC-907 may be developed into a possible therapeutic approach for patients with NB.

## Introduction

Neuroblastoma (NB) is the most common extracranial solid tumor affecting children, accounting for 7% of all tumors in children <15 years of age and 15% of all childhood cancer-related deaths (1). NB is a complex tumor with unique characteristics, and its biological heterogeneity leads to various clinical manifestations (2). Despite the aggressive multi-method treatment in high-risk NB cases, the 5-year survival rate of patients is <50%. At present, monoclonal GD2 specific antibodies have significantly improved the survival rates of patients with high-risk NB (3,4); however, the high costs associated with the use of GD2 monoclonal antibody for immunotherapy hinders its widespread use in patients in low- and middle-income countries. Given the limited number of frequently mutated genes in NB, the mode of targeted therapy against mutated oncogenes is challenging (5). Currently, numerous scholars have turned their attention to epigenetic drug therapy.

Histone deacetylase (HDAC) is an enzyme that regulates gene expression by remodeling chromatin structure. The dysregulation of HDAC expression leads to an imbalance of histone acetylation and promotes various human tumors (6), including NB (7). HDAC inhibitors (HDACis) have been confirmed to inhibit NB cell proliferation, and to induce differentiation, apoptosis and cell cycle arrest (8). Additionally, the combination of HDACis with other chemotherapeutic agents or radiation therapy has also recently been investigated in preclinical research and clinical trials of patients with NB (9,10).

CUDC-907 is a dual-target inhibitor of PI3K and HDAC, which has significant potential to inhibit tumor growth and metastasis by simultaneously destroying multiple oncogenic signal networks (11). Previous studies have demonstrated that

---

*Correspondence to:* Dr Feifei Sun or Dr Yi Que, Department of Pediatric Oncology, Sun Yat-sen University Cancer Center, 651 Dongfeng Road, Guangzhou, Guangdong 510060, P.R. China  
E-mail: sunff@sysucc.org.cn  
E-mail: queyi@sysucc.org.cn

\*Contributed equally

**Key words:** neuroblastoma, CUDC-907, histone deacetylase, PI3K, stem-like properties, pentraxin 3, CD44

CUDC-907 exerts inhibitory effects on various tumors (12-16). Currently, CUDC-907 has been investigated in phase I and II clinical trials for the treatment of multiple myeloma (NCT01742988) and relapsed/refractory diffuse large B-cell lymphoma (NCT01742988) (17,18). In the present study, we aimed to explore the anticancer effects of CUDC-907 on NB *in vivo* and *in vitro*, and to further investigate the mechanisms through which CUDC-907 affects cancer-promoting pathways and the stemness phenotype of NB cells. It is hoped that the findings presented herein may provide a promising approach and prospects for the treatment of NB.

## Materials and methods

**Study compound.** CUDC-907 was purchased from TargetMol. The drug powder was dissolved into a 10 mg/ml storage solution with an appropriate amount of dimethyl sulfoxide (DMSO), stored at  $-80^{\circ}\text{C}$ . *In vivo*, CUDC-907 was diluted into suspension by normal saline using an ultrasonic processor (QSONICA SonicatorQ700).

**Cells and cell culture.** All cell lines, including SK-N-SH, SK-N-BE(2), SH-SY5Y, SK-N-AS and IMR32, were purchased from Cobioer Biosciences Co., Ltd. The SK-N-SH and IMR32 cells were cultured in minimum essential medium (MEM; Gibco; Thermo Fisher Scientific, Inc.) supplemented with 10% fetal bovine serum (FBS; Gibco; Thermo Fisher Scientific, Inc.) and 1% 1 mM sodium pyruvate (Gibco; Thermo Fisher Scientific, Inc.) and 1% MEM non-essential amino acids (MEM NEAA; Gibco; Thermo Fisher Scientific, Inc.). The SK-N-BE(2) and SH-SY5Y cells were cultured in MEM/F12 (1:1) (Gibco; Thermo Fisher Scientific, Inc.) supplemented with 10% FBS, 1% 1 mM sodium pyruvate and 1% MEM NEAA. The SK-N-AS cells were cultured in Dulbecco's modified Eagle's medium (DMEM; Gibco; Thermo Fisher Scientific, Inc.) supplemented with 10% FBS. All culture mediums were supplemented with 1% penicillin-streptomycin solution (Gibco; Thermo Fisher Scientific, Inc.). All cells were cultured in a 5%  $\text{CO}_2$  and humidified incubator maintained at  $37^{\circ}\text{C}$ . All cell lines had been authenticated by STR profiling.

**Cell Counting Kit-8 (CCK-8) assay.** CUDC-907 at the initial maximum concentration (2 mM) was diluted at a gradient ratio of 1:10 in 96-well plates with adherent cells. The blank control group received DMSO instead of CUDC-907. In addition, each well was provided with three vice-holes. Moreover, 10  $\mu\text{l}$  CCK-8 (ApexBio) was added to each well of the plate. The absorbance at 450 nm was measured using a microplate reader (Tecan Spark 10M, Tecan Group, Ltd.) after incubating at  $37^{\circ}\text{C}$  for 2 h.

**Colony formation assay.** The cells were prepared into a cell suspension at a concentration of  $2 \times 10^3/\text{ml}$ . After 24 h, an appropriate amount of PBS was added for washing. Medium containing various concentrations (2, 4, 8 and 16 nM) of CUDC-907 was then added, and each well was provided with three vice-holes. The cells were incubated at  $37^{\circ}\text{C}$  in the 5%  $\text{CO}_2$  humidified incubator for 10-14 days. Following removal from the incubator, the cells were fixed with 10%

formalin (Biosharp Life Sciences) for 20 min, and then stained with crystal violet (MilliporeSigma) for 10 min, with both procedures conducted at room temperature.

**Apoptosis analysis.** The apoptosis of NB cells treated with or without CUDC-907 was analyzed using flow cytometry. All the procedures were performed following the manufacturer's instructions (Annexin V-FITC/PI Kit, 4A Biotech, Co., Ltd.). Briefly, a total of  $5 \times 10^5$  NB cells were prepared, washed in PBS twice, and then resuspended with 500  $\mu\text{l}$  binding buffer. The cells were then incubated with 5  $\mu\text{l}$  Annexin V-FITC for 15 min in the dark at room temperature, and 5  $\mu\text{l}$  propidium Iodide (PI) was then added to each tube. The stained cells were then analyzed using a flow cytometer (CytoFLEX, Beckman Coulter, Inc.) within 1 h.

**Western blot analysis.** Whole-cell lysates were generated using RIPA lysis buffer (Thermo Fisher Scientific, Inc.), and the protein concentration was detected using a BCA kit (Thermo Fisher Scientific, Inc.). An equal amount of protein was separated using 10% SDS-PAGE and then transferred onto polyvinylidene fluoride (PVDF) membranes. After blocking in 5% skim milk (EpiZyme) for 1 h at room temperature, the PVDF membranes were incubated overnight with primary antibodies at  $4^{\circ}\text{C}$ , followed by incubation with secondary antibodies for 2 h at room temperature. All the antibodies used are listed in Table SI. Signal detection was conducted using the ECL chemiluminescence detection system (Bio-Rad Laboratories, Inc.).

**Reverse transcription-quantitative PCR (RT-qPCR).** Total RNA was extracted from the cultured NB cells using TRIzol reagent (Ambion; Thermo Fisher Scientific, Inc.). RNA was reverse transcribed using the RT001 Fast Reverse Transcription kit (ES-RT001, ES Science). qPCR was then performed on the Bio-Rad CFX96 (Bio-Rad Laboratories, Inc.) with SYBR-Green Master Mix (ES-QP002, ES Science). The primers used are listed in Table SII. The amplification reactions were conducted using the following cycling parameters  $95^{\circ}\text{C}$  for 10 min, followed by 40 cycles of  $95^{\circ}\text{C}$  for 10 sec, and  $60^{\circ}\text{C}$  for 30 sec. The  $2^{-\Delta\Delta\text{Ct}}$  method was used to calculate the levels of gene expression (19).

**Matrigel invasion assay.** Transwell inserts (BD Biosciences) coated with 50  $\mu\text{l}$  Matrigel were used for the Matrigel invasion assay as previously described (20).

**Wound healing assay.** The NB cells at a density of  $10^5$  cells/ml were cultured in 6-well plates with scratch plug-in components. The protocol of the wound healing assay was as previously described (20).

**Sphere formation assay.** FBS-free DMEM/F12 supplemented with 2% B27 (Invitrogen; Thermo Fisher Scientific, Inc.), 20 ng/ml human recombinant EGF (Invitrogen; Thermo Fisher Scientific, Inc.) and 20 ng/ml bFGF (Invitrogen; Thermo Fisher Scientific, Inc.) were used for the sphere formation experiment. A total of 300 SK-N-BE(2) cells suspended in tumor sphere medium were seeded into each ultra-low attachment 24-well plate for 14 days. After forming spheres, the cells were

transferred to another new 24-well plate for further culture and different generations of sphere-forming cells were collected for RT-qPCR assays.

**Patients and specimens.** A total of 55 patients included in the present study were newly diagnosed with NB in the Sun Yat-sen University Cancer Center between April, 2009 to June, 2016. These patients were between 10 to 179 months old, and the median age was 45 months, with 25 females and 30 males. The selection criteria for enrolling patients were as follows: i) A pathological diagnosis of NB; ii) an age <18 years; iii) tissue specimens were obtained prior to the initiation of treatment; and iv) a complete and detailed treatment process and follow-up data. The specimens from patients with NB were obtained by needle biopsy or open surgery. The research protocol was approved by the Institutional Review Board (IRB) of the Sun Yat-sen University Cancer Center (SYSUCC; Guangzhou, China; approval no. B2021-274-01). Informed written consent was obtained from the parents of each patient involved in the study.

**Immunohistochemistry (IHC).** The NB tissue specimens were fixed in formalin, embedded in paraffin blocks, and sectioned at a thickness of 4  $\mu$ m. IHC was performed following standard protocols. The sections were blocked with 5% goat serum (C0265, Beyotime Institute of Biotechnology) at room temperature for 30 min. They were then incubated with primary antibodies against Ki67 (1:500; cat. no. ab92742, Abcam), HDAC1 (1  $\mu$ g/ml; cat. no. ab19845, Abcam), HDAC2 (1:1,000; cat. no. ab32117, Abcam), HDAC3 (1:500; cat. no. ab32369, Abcam), CD44 (1:200; cat. no. sc-7297, Santa Cruz Biotechnology, Inc.) at 4°C. The following day, the sections were washed in PBS three times and then incubated with goat anti-rabbit secondary antibody (HRP-conjugated, 1:200; cat. no. CW0103S, CWBio) or goat anti-mouse secondary antibody (HRP-conjugated, 1:200; cat. no. CW0102S, CWBio) for 2 h at room temperature. The results were evaluated according to the staining intensity and the proportion of tumor cells with an unequivocal positive reaction. The intensity was scored as follows: 0, negative; 1, weak; 2, moderate; and 3, strong. The frequency of positive cells was defined as follows: 0, <5%; 1, 5-25%; 2, 26-50%; 3, 51-75%; and 4, >75%. The composite score was the product of the two scores. The composite scores of 0 to 7 were considered a low expression, and 8 to 12 were considered a high expression. A fluorescence microscope (Olympus BX61, Olympus Corporation) was used for image acquisition and two independent pathologists reviewed the slides and evaluated the scores.

**Luciferase assay.** Human CD44 expression plasmids purchased from Guangzhou iGene Biotechnology Co., Ltd. were transfected into SK-N-BE(2) cells using Lipofectamine 3000<sup>®</sup> (Thermo Fisher Scientific, Inc.) for 48 h. The cells were then treated with culture medium containing CUDC-907 for 24 h. Subsequent procedures of assay were conducted using the Dual-Luciferase Reporter Gene Assay kit (DL101-01, Vazyme Biotech Co., Ltd.) following the manufacturer's protocol. A total of 20  $\mu$ l cell extract was mixed with 100  $\mu$ l luciferase assay reagent at room temperature and the reaction was detected with a microplate reader (Tecan Spark 10M,

Tecan Group, Ltd.). The ratio of Firefly to *Renilla* Luciferase activity was calculated for each hole.

**Xenograft tumorigenesis in vivo.** All the animal experiments were carried out in accordance with the Animal Care and Use Committee of the Sun Yat-sen University Cancer Center, and were approved by the Animal Ethics Committee of Sun Yat-sen University (Approval no. L102042020120P). A mixture of SK-N-BE(2) cell suspension ( $8 \times 10^6$  cells) and thawed Matrigel (Corning, Inc.) was injected subcutaneously into the right inguinal of 14 female NOD/SCID mice, aged 3-4 weeks (GemPharmatech), weighing between 15 to 20 g, in a SPF environment (room temperature, 20-26°C; relative humidity, 40-70%; alternating time for the light/dark cycle, 12/12 h; food and water were regularly provided by the feeders). Subcutaneous tumor formation was palpable in 12 mice after 1 week, and the mice were then randomly divided into a control group and a treatment group, with 6 mice in each group. The treatment group was administered with 100  $\mu$ l CUDC-907 solution (25 mg/kg) via gavage for 5 days, and the treatment was continued for 5 days after an interval of 2 days. The control (vehicle) group was administered with 100  $\mu$ l normal saline via gavage at the same time. During this period, the body weight and tumor volumes of the mice were measured and recorded every 2 days, and tumor volumes were calculated using the formula  $V = (\text{short diameter}^2 \times \text{long diameter}) / 2$ . Following a total of 10 days of treatment, the mice were euthanized with carbon dioxide using the displacement rate at 50% volume per minute (21), and the subcutaneous tumors were removed to measure their size and weight. When the tumor diameter of any mice reached 2 cm, this was regarded as the humane endpoint in this experiment.

**Small interfering RNA (siRNA) transfection and lentiviral transduction.** The detailed procedures for siRNA transfection and lentiviral transduction of the NB cells were as previously described (20). Human siRNA oligos targeting PTX3 were purchased from Shanghai GenePharma Co., Ltd, at a working concentration of 50 nM. The siRNA sequences were as follows: siNC, UUCUCCGAACGUGUCACGUTT (5'-3') and TTAAGAGGCUUGCACAGUGCA (3'-5'); siPTX3#1, GCA CAAAGAGGAAUCCAUATT (5'-3') and UAUGGAUUC CUCUUUGUGCTT(3'-5'); siPTX3#2, GGGAUAGUGUUC UUAGCAATT (5'-3') and UUGCUAAGAACACUAUCC CTT (3'-5'). The PTX3 overexpression plasmids and lentiviral vectors were purchased from GeneCopoeia.

**RNA sequencing (RNA-seq) and data analysis.** The cells were treated with DMSO or CUDC-907 at 25 nM for 24 h, and total RNA was extracted using TRIzol<sup>®</sup> reagent (Invitrogen; Thermo Fisher Scientific, Inc.). The cDNA library building and RNA-seq were performed using a commercially available service (service ID F21FTSSCWJ1037, BGI, Huada Biotechnology). RNA-seq reads were aligned to the hg38 genome. Differentially expressed genes (DEGs) were identified using  $|\log_2FC| \geq 1$  and  $FDR \leq 0.001$ .

**Statistical analysis.** All the experiments were performed in triplicate. Data are expressed as the mean  $\pm$  standard deviation, and comparisons between groups were performed using

an unpaired Student's t-test or one-way ANOVA followed by Tukey's post hoc test. Fisher's exact test was used to assess the association between HDACs or the CD44 expression level and clinicopathological variables. Kaplan-Meier curves were used for survival analysis following the log-rank test. Overall survival (OS) was defined as the endpoint of the study as the period from the date of initial diagnosis to mortality or the last follow-up. Event-free survival (EFS) was defined as the period from the date of the initial diagnosis to the date of recurrence, progression, mortality, or a second malignancy.  $P < 0.05$  was considered to indicate a statistically significant difference. All the data was analyzed using SPSS 25.0 software (IMB Corp.) or GraphPad Prism 8.0 software (Graphpad Software, Inc.).

## Results

*CUDC-907 inhibits the proliferation, induces the apoptosis, and suppresses the migratory ability of NB cells.* CUDC-907 is a dual target inhibitor of HDAC and PI3K. The present study evaluated the effects of CUDC-907 on the viability of five NB cell lines, including MYCN non-amplified NB cell lines (SK-N-SH, SH-SY5Y and SK-N-AS) and MYCN-amplified NB cell lines [SK-N-BE(2) and IMR32]. The results revealed that CUDC-907 inhibited the viability of the five NB cell lines in a concentration-dependent manner within 72 h, and the half-maximal inhibitory concentration (IC<sub>50</sub>) values calculated by GraphPad Prism ranged from 5.53 to 46.22 nM (Fig. 1A and B). The colony formation assay revealed that cell proliferation was significantly inhibited by CUDC-907 (Fig. 1C). Subsequently, flow cytometric analysis was performed and it was found that CUDC-907 significantly induced apoptosis (Fig. S1A). The results of western blot analysis demonstrated an increased expression of Bax, Bak and cleaved caspase-3, and a decreased protein expression of Bcl-2 in the cells treated with CUDC-907 (Fig. 1D). Furthermore, the inhibitory effects of CUDC-907 on the migratory ability of NB cells were also demonstrated by the wound healing assay (Fig. S1B) and the Matrigel invasion assay (Fig. S1C).

*CUDC-907 inhibits the growth of NB xenografts in vivo.* The potential anti-NB effect of CUDC-907 was explored *in vivo*. The detailed mode of administration is illustrated in Fig. 2A. Following treatment for 10 days, CUDC-907 significantly inhibited NB tumor growth and weight compared with the vehicle control (Fig. 2B, D and E), while there was no significant difference in the body weight of the mice in the two groups (Fig. 2C). The results of western blot analysis (Fig. 2F) revealed that CUDC-907 markedly increased H3K27ac expression, whereas it inhibited the expression of phosphorylated (p-)AKT. IHC staining revealed that CUDC-907 downregulated the expression of the proliferative marker, Ki67, compared to the control tissues (Fig. 2G and H).

*CUDC-907 downregulates MYCN expression, and suppresses the activation of the PI3K/AKT and MAPK/ERK pathways in NB cells.* MYCN amplification is associated with the poor prognosis of patients with NB (22); thus, the present study investigated whether CUDC-907 downregulates the expression of MYCN. The two MYCN-amplified cell lines, SK-N-BE(2) and IMR32, exhibited higher MYCN mRNA and protein levels

compared to the MYCN non-amplified cell lines, SK-N-SH, SH-SY5Y and SK-N-AS (Fig. 3A and B). The SK-N-BE(2) or IMR32 cells were treated with CUDC-907 at the indicated concentrations (0, 10, 25, 50 and 100 nM) for 24 h, or with a fixed concentration of 50 nM for various periods of time (0, 2, 4, 6, 16, 24 and 48 h) to observe the changes in MYCN protein levels. The results revealed that CUDC-907 downregulated MYCN expression in a concentration- and time-dependent manner in the MYCN-amplified NB cell lines (Fig. 3C-F).

Furthermore, the downstream targets directly regulated by CUDC-907 were verified. The results revealed that H3K27ac expression was markedly increased in the NB cell lines, SK-N-SH, SK-N-BE(2) and IMR32, following exposure to CUDC-907 for 24 h. Moreover, the expression of p-AKT, which is downstream of activated PI3K, was also obviously decreased (Fig. 3G). Activating mutations in the RAS-MAPK-ERK pathway are known to occur at a high frequency in relapsed NB (23,24). Thus, the present study examined the changes in the downstream proteins of MAPK, p-MEK/MEK and p-ERK/ERK, and found that the p-ERK expression level was markedly decreased by CUDC-907 (Fig. 3G).

*CUDC-907 inhibits the stem-like properties of NB by inhibiting PTX3.* Cancer stem cells (CSCs) lead to post-transplant relapse and are associated with poor survival outcomes of patients with high-risk NB (25,26). Herein, to explore whether CUDC-907 affects the stem cell-like properties of NB, a sphere formation assay was performed using the SK-N-BE(2) cells exposed to the indicated concentrations (0, 2, 4, 8 and 16 nM) of CUDC-907. Following treatment of the SK-N-BE(2) cells with 4, 8 or 16 nM CUDC-907, clonogenic formation exhibited a marked decrease compared to the controls in concentration-dependent manner (Fig. 4A and B). Furthermore, both the mRNA and protein levels of several stem cell markers, including CD44, SOX2, OCT4 and BMI-1, were significantly downregulated by CUDC-907 (Fig. 4C and D).

To further explore the mechanisms through which CUDC-907 affects the stem-like properties of NB cells, RNA-seq analysis was performed using two NB cell lines [SK-N-BE(2) and SK-N-SH]. According to the DEGs painted into a heatmap, 20 DEGs were identified (Fig. S1D), of which PTX3 was the only downregulated gene. CUDC-907 significantly inhibited the expression of PTX3 at the mRNA level in NB cells (Fig. 5A). PTX3 is a ligand and upstream protein of CD44, which has been identified as a CSC marker in several types of cancer, including NB (27-29). PTX3 has also been reported to promote the stemness of breast cancer cells by activating the downstream ERK1/2, AKT and NF- $\kappa$ B pathways (30); however, its role in NB has not been reported to date, at least to the best of our knowledge. In the present study, PTX3 siRNA was transfected into SK-N-BE(2) cells to knockdown PTX3 expression. It was observed that PTX3 knockdown significantly decreased the expression of CD44 and that of a series of other stemness-associated genes, as well as tumor sphere forming ability of the cells (Fig. 5B-E). Even though previous research has indicated that PTX3 activates the AKT pathway (30), the present study revealed that the level of p-AKT did not exhibit any obvious change following the knockdown of PTX3. This discrepancy may be attributed to the different functions of PTX3 in various cell types; thus,

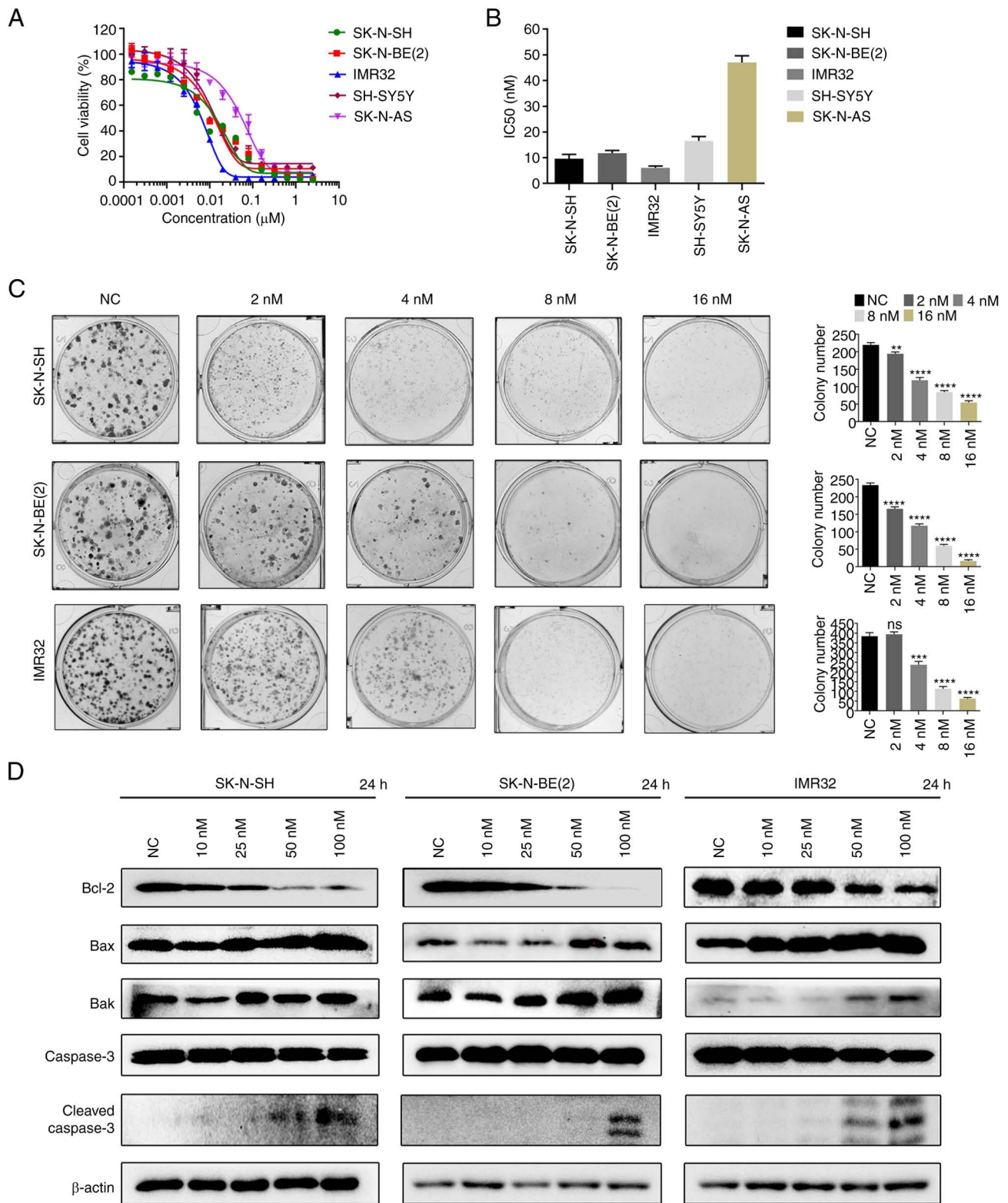


Figure 1. CUDC-907 inhibits the proliferation, induces the apoptosis, and reduces the migratory ability of NB cells. (A and B) The indicated NB cell lines were treated with various concentrations of CUDC-907, and the IC<sub>50</sub> value was calculated at 72 h. Data are presented as the mean  $\pm$  SD. (C) Effect of various concentrations of CUDC-907 on the colony formation of SK-N-SH, SK-N-BE(2) and IMR32 cells. The histogram on the right indicates the number of clones. \*\* $P < 0.01$ , \*\*\* $P < 0.001$  and \*\*\*\* $P < 0.0001$ , vs. NC; ns, not significant. (D) SK-N-SH, SK-N-BE(2) and IMR32 cells were collected for western blot analysis with the indicated antibodies against apoptosis-related proteins following treatment with various concentrations of CUDC-907 for 24 h. NB, neuroblastoma; NC, negative control.

these findings need to be verified in future studies. In addition, it was found that the reduction of sphere formation and CD44 mRNA/protein expression by CUDC-907 was reversed

by exogenous PTX3 overexpression (Fig. 5F-I). These findings indicated that CUDC-907 inhibited the stem-like properties of NB cells and CD44 expression by inhibiting PTX3.

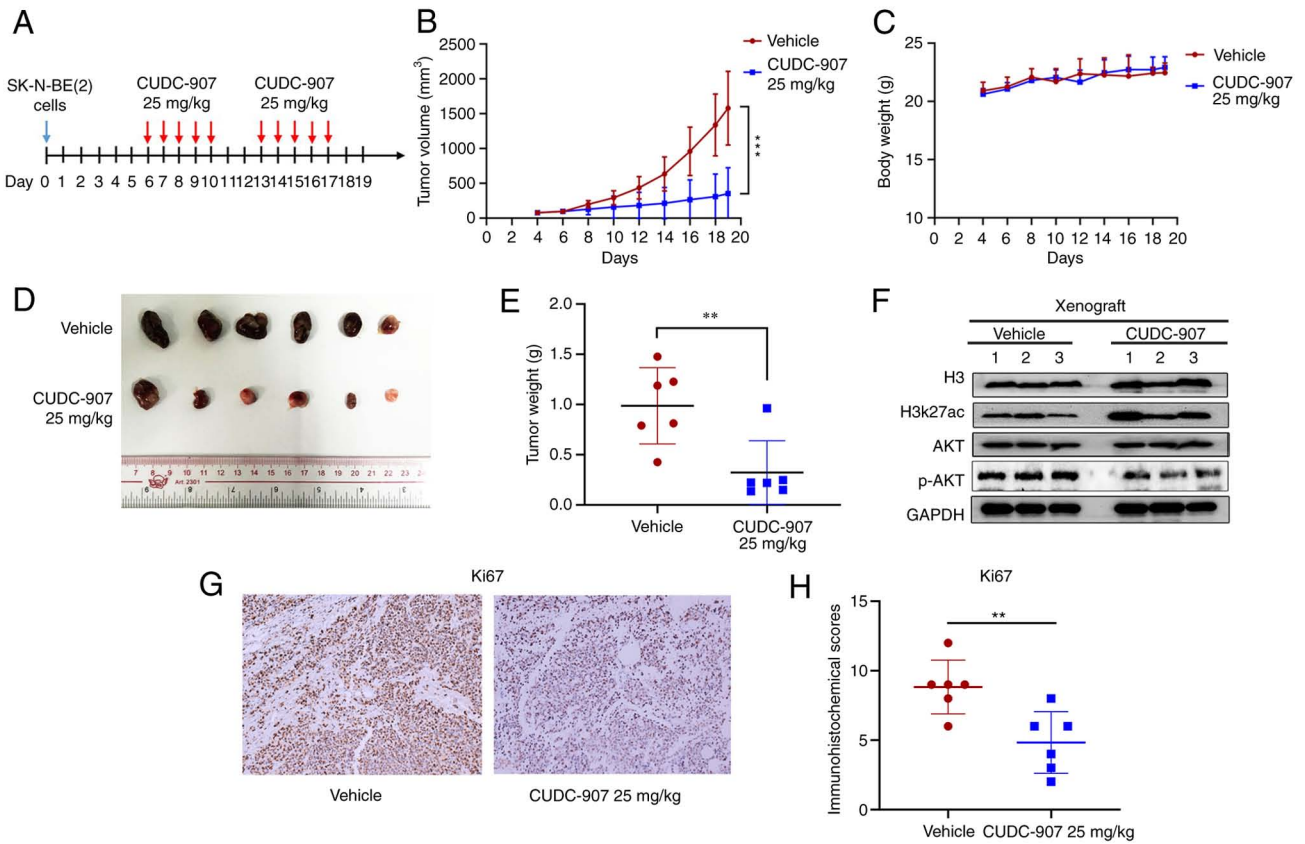


Figure 2. CUDC-907 inhibits the growth of NB xenografts *in vivo*. (A) Schematic diagram illustrating the administration mode and time in mice. The curves of (B) relative tumor volume and (C) body weight of the mice treated with CUDC-907 or the vehicle. Error bars represent the mean  $\pm$  SD in each group. \*\*\* $P < 0.001$ . Comparison of (D) tumor size and (E) tumor weight between the vehicle and CUDC-907-treated group. \*\* $P < 0.01$ . (F) Changes in the protein levels of H3, H3K27ac, AKT and p-AKT in the animal tissues between the vehicle and CUDC-907-treated group. (G and H) Changes in Ki67 expression in NB tissues between the vehicle and CUDC-907-treated group. \*\* $P < 0.01$ . NB, neuroblastoma; H3, histone H3.

*High expression of HDAC1, 2, 3 and CD44 is associated with the poor prognosis of patients with NB.* To observe whether the target proteins of CUDC-907 are associated with the prognosis of patients with NB, IHC of HDAC1, 2, 3 and CD44 was performed on paraffin-embedded sections of 55 patients with NB from Sun Yat-sen University Cancer Center (Fig. 6A). The median follow-up time was 38.9 months (range, 9.6 to 124.6 months). Up to the final follow-up date, 17 patients (30.9%) succumbed and 33 patients (60.0%) suffered disease progression or recurrence.

The association between HDAC1, 2, 3 expression and the clinical characteristics of patients with NB was analyzed (Tables SIII-SV). The results revealed that the expression level of HDAC3 was related to MYCN amplification (OR, 15.789;  $P = 0.002$ ), the International Neuroblastoma Staging System (INSS) staging system (OR, 6.400;  $P = 0.043$ ) and the Children's Oncology Group (COG) risk group (OR, 7.243;  $P = 0.017$ ) (Table SV). Kaplan-Meier survival analysis indicated that the upregulated mRNA levels of HDAC1, HDAC2 and HDAC3 were significantly associated with a poor OS (HDAC1,  $P = 0.0209$ ; HDAC2,  $P = 0.0143$ ; HDAC3,  $P = 0.0063$ ) and EFS (HDAC1,  $P = 0.0023$ ; HDAC2,  $P = 0.0026$ ; HDAC3,  $P = 0.0309$ ) (Fig. 6B-G). It was also found that the high expression of CD44 was significantly associated with a poor OS ( $P = 0.0239$ ) and EFS ( $P = 0.0477$ ) of patients with NB (Fig. 6H and I). However, the high expression of CD44 was found not to be significantly

associated with the clinical characteristics of patients with NB (Table SVI).

## Discussion

NB is one of the most common extracranial solid tumors affecting children. More than half of patients with NB are initially diagnosed with high-risk disease and have a poor prognosis. Although immunotherapy with GD2 monoclonal antibody is available, 30-40% of high-risk patients still ultimately succumb due to tumor progression (31). The literature demonstrates that HDACs are abnormally highly expressed in NB tissues, and pan-HDACs exert potent antitumor effects on NB cells *in vitro* (7). Moreover, the pathological activation of AKT frequently occurs in NB and is associated with a poor prognosis (32), and upstream PI3K signaling play a crucial role in NB cell growth/survival (33,34). Thus far, either HDACs or PI3K inhibitors as monotherapy have not been particularly successful in clinical trials (35-37). CUDC-907, as a dual-target inhibitor of HDAC and PI3K, synergistically enhances the antitumor activity in lymphomas (12,17), acute myeloid leukemia (13), chronic lymphocytic leukemia (14), pancreatic cancer (15) and high-grade glioma (16), indicating its promising role in the treatment of human tumors. However, its specific effect and the underlying regulatory mechanisms in NB remain

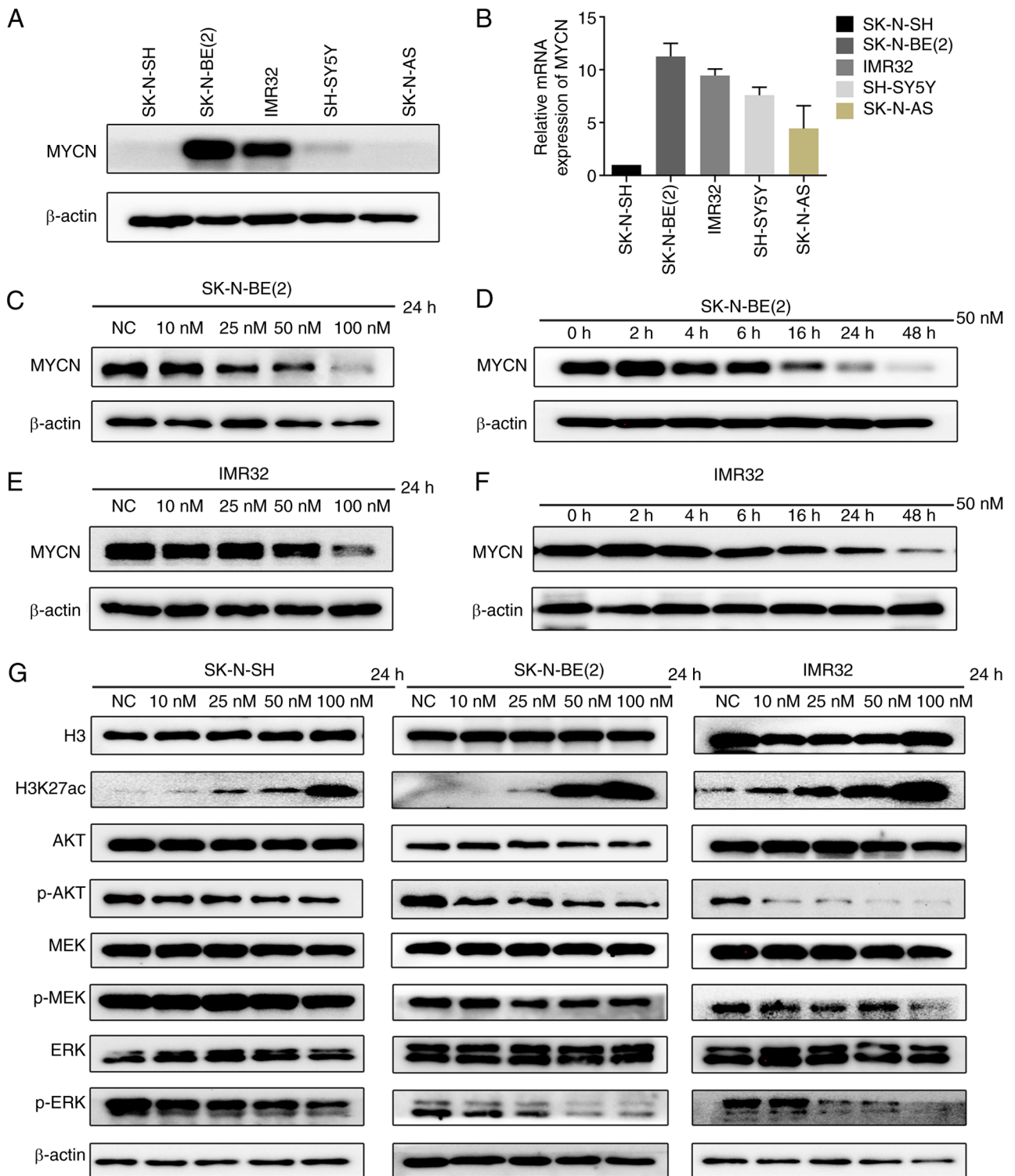


Figure 3. CUDC-907 downregulates MYCN expression, and suppresses the activation of the PI3K/AKT and MAPK/ERK pathways in NB cells. (A) Western blot analysis and (B) reverse transcription-quantitative PCR of MYCN expression in the indicated NB cells. (C and D) Western blot analysis of MYCN expression in SK-N-BE(2) cells treated (C) with various concentrations of CUDC-907 for 24 h or (D) with a fixed concentration of CUDC-907 (50 nM) for the indicated periods of time. (E and F) Western blot analysis of MYCN expression in IMR32 cells treated (E) with various concentrations of CUDC-907 for 24 h or (F) with a fixed concentration of CUDC-907 (50 nM) for the indicated periods of time. (G) Western blot analysis of H3K27ac, AKT, p-AKT, MEK, p-MEK, ERK and p-ERK expression in the SK-N-SH, SK-N-BE(2) and IMR32 cells treated with various concentrations of CUDC-907 for 24 h. NB, neuroblastoma; H3, histone H3.

unclear. Although Chilamakuri *et al* (38) evaluated the antitumor effects of CUDC-907 on NB cells *in vitro*, the present study found that CUDC-907 significantly inhibited the stem-like properties of NB cells, which has not been

reported to date, at least to the best of our knowledge. The present study further explored the effects of CUDC-907 on NB *in vitro* and *in vivo*, as well as its potential mechanisms, to discover promising clinical drugs for targeted therapy.

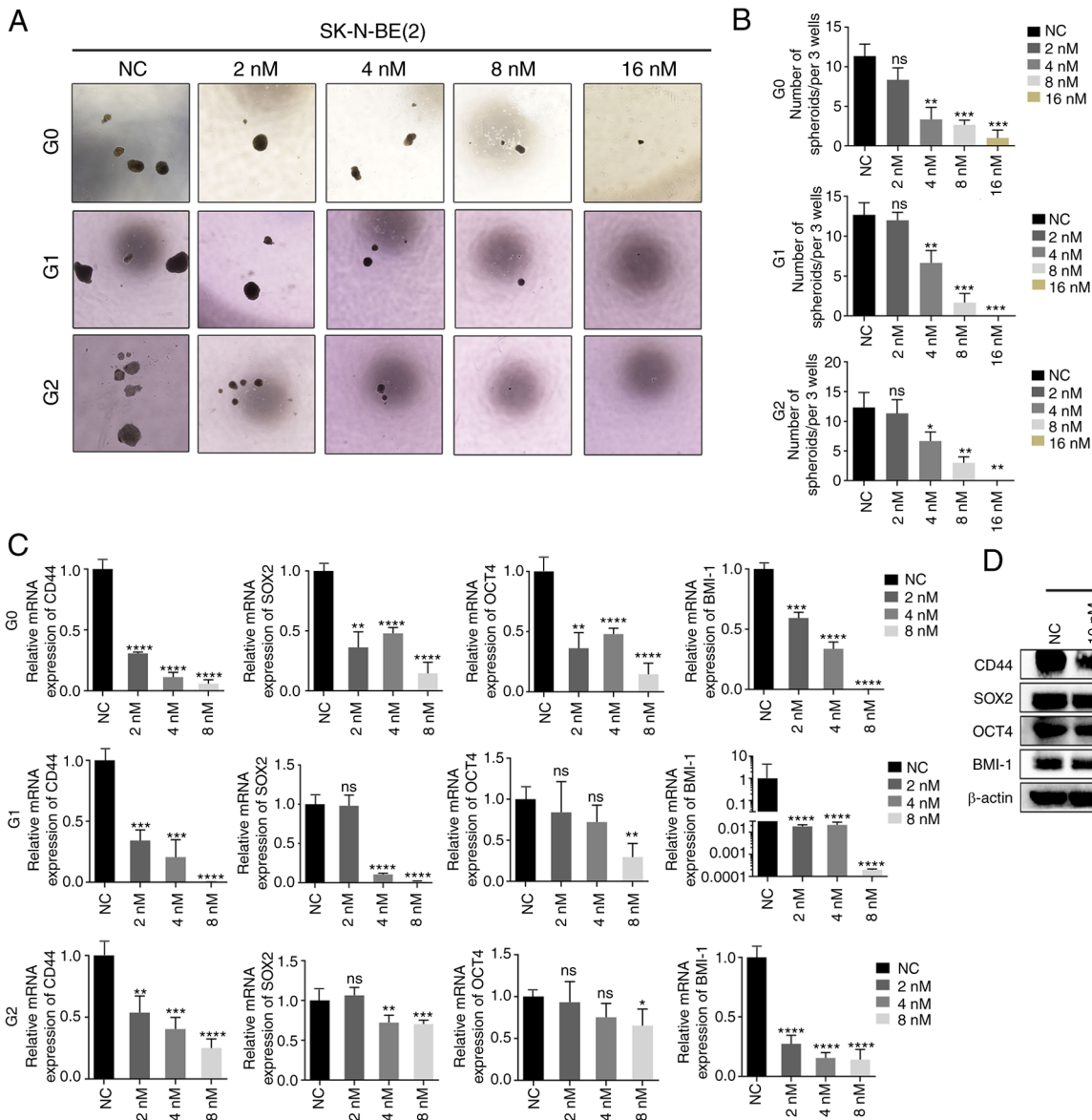


Figure 4. NB cells treated with CUDC-907 exhibit weaker CSC-like properties. (A) Sphere images of the first, second and third generation of SK-N-BE(2) cells treated with various concentrations of CUDC-907. (B) The sphere numbers of the first, second and third generation of SK-N-BE(2) cells treated with various concentrations of CUDC-907. \* $P < 0.05$ , \*\* $P < 0.01$  and \*\*\* $P < 0.001$ ; ns, not significant. (C) Reverse transcription-quantitative PCR of the expression of the stem cell markers, CD44, SOX2, OCT4 and BMI-1, in the first, second and third generation of SK-N-BE(2) cells treated with the indicated concentrations of CUDC-907. \* $P < 0.05$ , \*\* $P < 0.01$ , \*\*\* $P < 0.001$  and \*\*\*\* $P < 0.0001$ , vs. NC group; ns, not significant. (D) Following CUDC-907 treatment, western blot analyses were performed on the indicated stem cell markers in SK-N-BE(2) cells at the protein level. NB, neuroblastoma; SOX2, sex determining region Y-box 2; OCT4, octamer-binding transcription factor 4; BMI-1, B-cell-specific Moloney murine leukemia virus integration site 1.

In the present study, it was verified that CUDC-907 significantly increased histone H3 acetylation and inhibited the phosphorylation of AKT in NB cells. Using CCK-8, colony formation, wound healing and Matrigel invasion assays, the inhibitory effects of CUDC-907 on the proliferation and migration of NB cells were illustrated. Through western blot analysis, it was verified that CUDC-907 promoted apoptosis in a concentration-dependent manner by regulating the Bcl-2 family and activating caspase-3.

In NB xenografts, it was confirmed that CUDC-907 significantly inhibited tumor growth, which was consistent with the reported studies revealing the antitumor effect of CUDC-907 *in vivo* (11-15). CUDC-907 has been shown to effectively inhibit the proliferation of a variety of tumor cells with an IC<sub>50</sub> value

of 0.7-120 nM, and the dosage used in mice is 25-300 mg/kg for oral administration. Qian *et al.* (11) and Mondello *et al.* (39) found that CUDC-907 (25, 50 and 100 mg/kg p.o.) significantly delayed the growth of transplanted tumors without significant toxicity. Based on these findings, the present study used a dose of 25 mg/kg for oral administration. Further studies with increased dosage groups and a positive control are expected in future studies.

In terms of the drug distribution after CUDC-907 enters the body, even though this was not explored in the present study, the experimental results using mice illustrated the effectiveness of CUDC-907 in NB animal models. Furthermore, there are already several clinical trials (NCT03002623, NCT02307240, NCT02674750, NCT02909777 and NCT01742988) evaluating

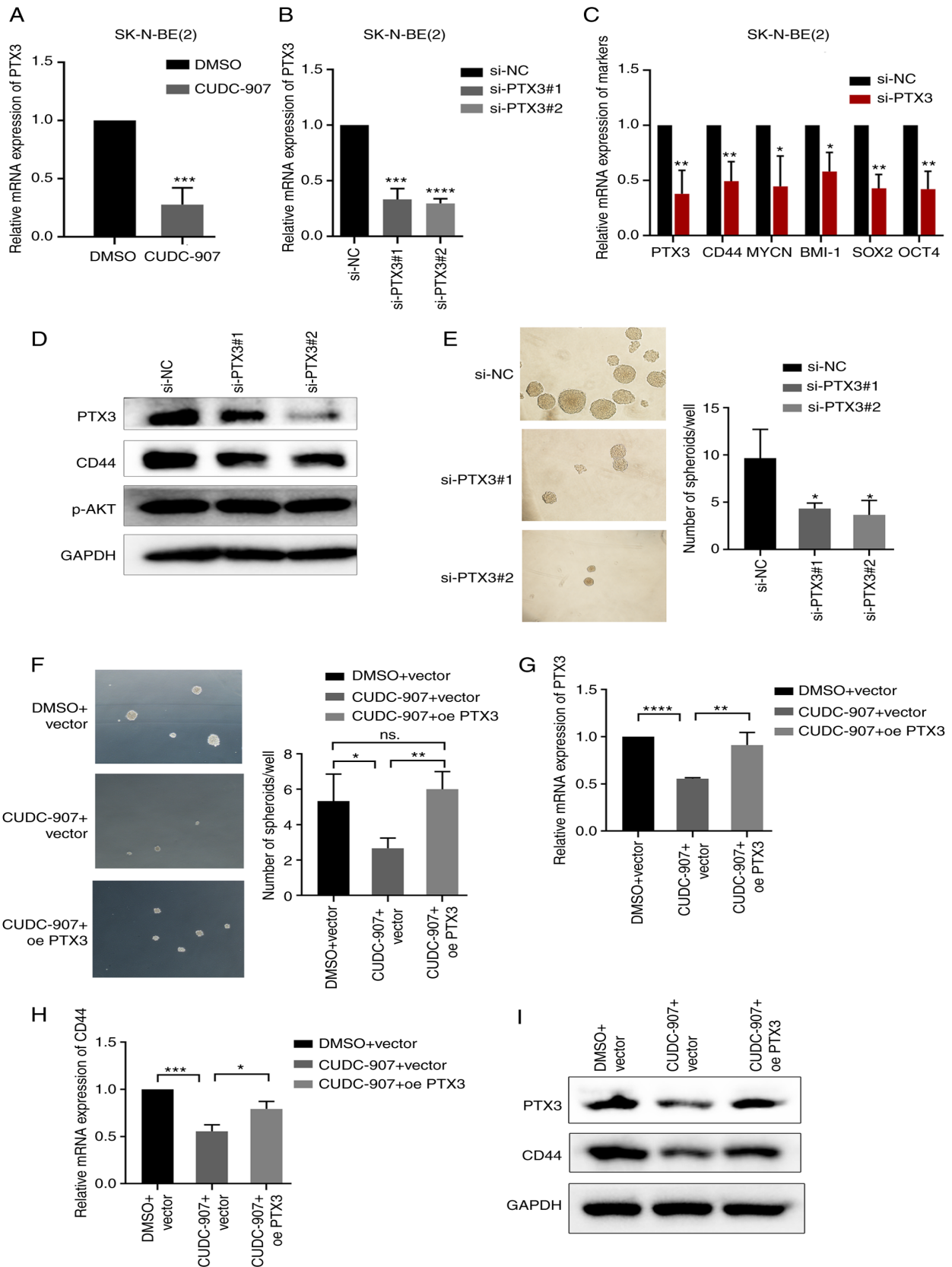


Figure 5. CUDC-907 inhibits the stem-like properties of NB by suppressing PTX3. (A) mRNA levels of PTX3 in cells treated with 50 nM CUDC-907 for 24 h. \*\*\* $P < 0.001$ , vs. DMSO control. (B) mRNA levels of PTX3 in cells transfected with PTX3 siRNA. \*\*\* $P < 0.001$  and \*\*\*\* $P < 0.0001$ , vs. negative control. (C) mRNA levels of PTX3, CD44, MYCN, BMI-1, SOX2 and OCT4 expression in cells transfected with negative control or PTX3 siRNA. \* $P < 0.05$  and \*\* $P < 0.01$ , vs. negative control. (D) PTX3, CD44 and p-AKT protein expression levels in cells transfected with PTX3 siRNA. (E) Sphere formation of empty vector-transfected cells exposed to DMSO, empty vector-transfected cells exposed to 50 nM CUDC-907 and PTX3-overexpressing cells exposed to 50 nM CUDC-907. \* $P < 0.05$  and \*\* $P < 0.01$ ; ns, not significant. (G-I) The mRNA/protein expression levels of PTX3 and CD44 in empty vector-transfected cells exposed to DMSO, empty vector-transfected cells exposed to 50 nM CUDC-907 and PTX3-overexpressing cells exposed to 50 nM CUDC-907. \* $P < 0.05$ , \*\* $P < 0.01$ , \*\*\* $P < 0.001$  and \*\*\*\* $P < 0.0001$ . NB, neuroblastoma; PTX3, pentraxin 3; SOX2, sex determining region Y-box 2; OCT4, octamer-binding transcription factor 4; BMI-1, B-cell-specific Moloney murine leukemia virus integration site 1.

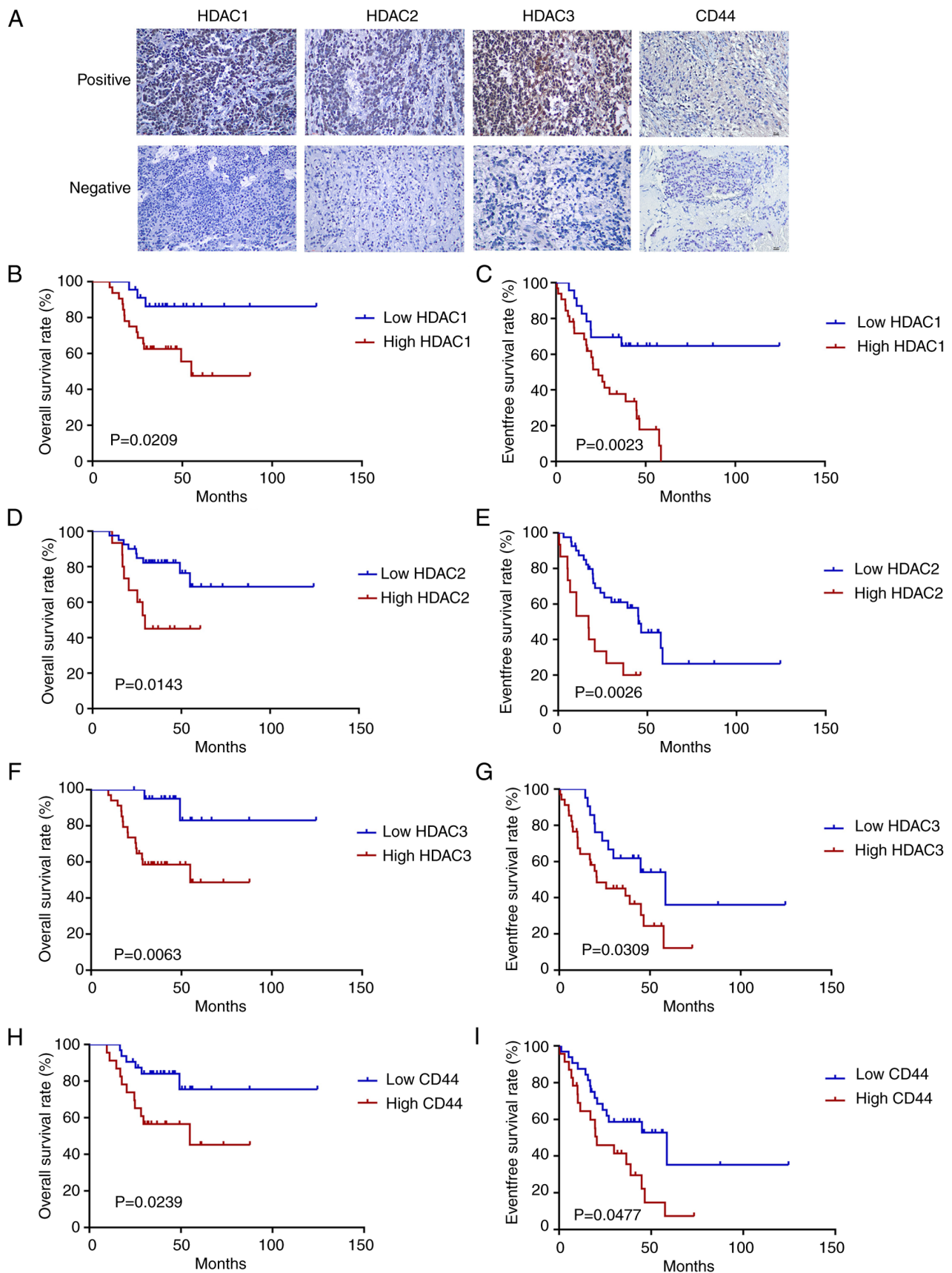


Figure 6. High expression levels of HDAC1, 2, 3 and CD44 are associated with a poor prognosis of patients with NB. (A) Immunohistochemistry images of the positive and negative expression of HDAC1, HDAC2, HDAC3 and CD44 in NB tissues. (B and C) The Kaplan-Meier survival curves of the OS or EFS of patients with NB based on HDAC1 expression levels ( $P=0.0209$  for OS and  $P=0.0023$  for EFS). (D and E) The Kaplan-Meier survival curves of the OS or EFS of patients with NB based on HDAC2 expression levels ( $P=0.0143$  for OS and  $P=0.0026$  for EFS). (F and G) The Kaplan-Meier survival curve of the OS or EFS of patients with NB based on HDAC3 expression levels ( $P=0.0063$  for OS and  $P=0.0309$  for EFS). (H and I) The Kaplan-Meier survival curve of the OS or EFS of patients with NB based on CD44 expression levels ( $P=0.0239$  for OS and  $P=0.0477$  for EFS). NB, neuroblastoma; HDAC, histone deacetylase; OS, overall survival; EFS, event-free survival.

the safety, tolerability and pharmacokinetics of CUDC-907 in human tumors, including NB (ClinicalTrials.gov), which will help to verify the safety and effective dose of CUDC-907 in human tumors.

MYCN amplification and gene mutations in the RAS-MAPK-ERK pathway are two of the most common genetic alterations related to recurrent NB. MYCN amplification has been shown to be associated with the poor prognosis of patients with NB, occurring in 25-30% of patients (25,40). The present study demonstrated that CUDC-907 significantly downregulated MYCN expression in a concentration- and time-dependent manner in MYCN-amplified NB cells. Previous studies have indicated that HDACs downregulate MYCN mRNA expression (41,42), while the PI3K/AKT/mTOR axis contributes to MYCN protein stabilization (43,44). Therefore, HDAC and PI3K antagonists may cooperate to inhibit the expression of MYCN in NB. It has been reported that 78% of mutations detected in relapsed NB are associated with the activation of the RAS-MAPK pathway (21,45). The aberrant regulation of the RAS-MAPK-ERK signaling pathway is critical for maintaining the self-renewal ability of CSCs, which promotes the proliferation, angiogenesis, metastasis and therapeutic resistance of NB cells, and also predicts the poor prognosis of patients with NB (46-48). In the present study, it was observed that the exposure of NB cells to CUDC-907 resulted in a decrease in p-ERK levels and in the suppression of the CSC phenotype in NB cells.

Based on the results of RNA sequencing, it was found that CUDC-907 inhibited the expression of PTX3 in SK-N-BE(2) and SK-N-SH NB cells. The secreted protein, PTX3, has been reported to be a partner of CD44 and promote the stem cell performance of tumor cells (30,49). CD44 is a transmembrane glycoprotein involved in cell-cell interactions and has been identified as a CSC and poor prognostic marker in various adult cancers (50-56) and pediatric cancers (57-60), including NB. However, the function of PTX3 and its association with CD44 in NB remains unknown. Herein, it was found that the knockdown of PTX3 using siRNA or its suppression using CUDC-907 weakened the sphere-forming ability and CD44 expression of the cells, both of which were reversed by the exogenous overexpression of PTX3. This indicated that CUDC-907 may reduce the stem like properties and CD44 stem cell marker expression via the inhibition of PTX3.

Finally, using the IHC of NB tissues, it was found that the high expression of HDAC1, HDAC2, HDAC3 and CD44 was associated with the poor prognosis of patients with NB, which indicated that HDACs or CD44 may be used as tumor biomarkers and potential therapeutic targets. However, a limitation of the present study was that the association between the expression levels of HDACs and CD44 was not explored. This needs to be investigated in future studies.

In conclusion, the present study demonstrates that CUDC-907 exerts a significant antitumor effect on NB, and may thus be worthy of further clinical development. Further studies are required to explore the role of CUDC-907 in NB and to provide more specific and accurate guidance for its translation into clinical practice.

#### Acknowledgements

Not applicable.

#### Funding

The present study was supported by the Key Technology Research Project of Guangzhou Science, Technology and Innovation Committee (grant no. 201902020001), the Guangzhou Science and Technology project (grant no. 201905010004), the National Scientific Foundation of China (grant no. 82002835) and the National Key Research and Development Program of China (grant no. 2022YFC2705005).

#### Availability of data and materials

The datasets used and/or analyzed during the current study are available from the corresponding author on reasonable request.

#### Authors' contributions

FS, YQ, YZ, ML and YHu conceived and designed the study. ML, YHu, YX and YHo conducted the experiments and collected the data. JW, LZ, SL, ZZ and JH analyzed and interpreted the data. YHu, ML, JW and FS were involved in the writing and preparation of the original draft. JZ and QL were involved in data curation and validation and were also involved in data analysis. ML, JW, YQ and YZ were involved in the reviewing, editing of the manuscript. YQ, FS and YZ were involved in funding acquisition. YHu and ML confirm the authenticity of all the raw data. All authors have read and agreed to the published version of the manuscript.

#### Ethics approval and consent to participate

The present study was approved by the Institutional Review Board (IRB) of the Sun Yat-sen University Cancer Center (SYSUCC; Guangzhou, China; approval no. B2021-274-01). Informed written consent was obtained from the parents of each patient involved in the study. All the animal experiments were carried out in accordance with the Animal Care and Use Committee of the Sun Yat-sen University Cancer Center, and were approved by the Animal Ethics Committee of Sun Yat-sen University (Approval no. L102042020120P).

#### Patient consent for publication

Not applicable.

#### Competing interests

The authors declared that they have no competing interests.

#### References

1. Maris JM, Hogarty MD, Bagatell R and Cohn SL: Neuroblastoma. *Lancet* 369: 2106-2120, 2007.
2. Whittle SB, Smith V, Doherty E, Zhao S, McCarty S and Zage PE: Overview and recent advances in the treatment of neuroblastoma. *Expert Rev Anticancer Ther* 17: 369-386, 2017.
3. Yu AL, Gilman AL, Ozkaynak MF, London WB, Kreissman SG, Chen HX, Smith M, Anderson B, Villablanca JG, Matthay KK, *et al*: Anti-GD2 antibody with GM-CSF, interleukin-2, and isotretinoin for neuroblastoma. *N Engl J Med* 363: 1324-1334, 2010.

4. McGinty L and Kolesar J: Dinutuximab for maintenance therapy in pediatric neuroblastoma. *Am J Health Syst Pharm* 74: 563-567, 2017.
5. Schramm A, Köster J, Assenov Y, Althoff K, Peifer M, Mahlow E, Odersky A, Beisser D, Ernst C, Henssen AG, *et al*: Mutational dynamics between primary and relapse neuroblastomas. *Nat Genet* 47: 872-877, 2015.
6. Mohammad HP, Barbash O and Creasy CL: Targeting epigenetic modifications in cancer therapy: Erasing the roadmap to cancer. *Nat Med* 25: 403-418, 2019.
7. Witt O, Deubzer HE, Lodrini M, Milde T and Oehme I: Targeting histone deacetylases in neuroblastoma. *Curr Pharm Des* 15: 436-447, 2009.
8. Robey RW, Chakraborty AR, Basseville A, Luchenko V, Bahr J, Zhan Z and Bates SE: Histone deacetylase inhibitors: Emerging mechanisms of resistance. *Mol Pharm* 8: 2021-2031, 2011.
9. Yin L, Liu Y, Peng Y, Peng Y, Yu X, Gao Y, Yuan B, Zhu Q, Cao T, He L, *et al*: PARP inhibitor veliparib and HDAC inhibitor SAHA synergistically co-target the UHRF1/BRCA1 DNA damage repair complex in prostate cancer cells. *J Exp Clin Cancer Res* 37: 153, 2018.
10. McClure JJ, Li X and Chou CJ: Advances and challenges of HDAC inhibitors in cancer therapeutics. *Adv Cancer Res* 138: 183-211, 2018.
11. Qian C, Lai CJ, Bao R, Wang DG, Wang J, Xu GX, Atayan R, Qu H, Yin L, Samson M, *et al*: Cancer network disruption by a single molecule inhibitor targeting both histone deacetylase activity and phosphatidylinositol 3-kinase signaling. *Clin Cancer Res* 18: 4104-4113, 2012.
12. Guo H, Zeng D, Zhang H, Bell T, Yao J, Liu Y, Huang S, Li CJ, Lorence E, Zhou S, *et al*: Dual inhibition of PI3K signaling and histone deacetylation halts proliferation and induces lethality in mantle cell lymphoma. *Oncogene* 38: 1802-1814, 2019.
13. Li X, Su Y, Madlambayan G, Edwards H, Polin L, Kushner J, Dzinic SH, White K, Ma J, Knight T, *et al*: Antileukemic activity and mechanism of action of the novel PI3K and histone deacetylase dual inhibitor CUDC-907 in acute myeloid leukemia. *Haematologica* 104: 2225-2240, 2019.
14. Chen Y, Peubez C, Smith V, Xiong S, Kocsis-Fodor G, Kennedy B, Wagner S, Balotis C, Jayne S, Dyer MJ and Macip S: CUDC-907 blocks multiple pro-survival signals and abrogates microenvironment protection in CLL. *J Cell Mol Med* 23: 340-348, 2019.
15. Fu XH, Zhang X, Yang H, Xu XW, Hu ZL, Yan J, Zheng XL, Wei RR, Zhang ZQ, Tang SR, *et al*: CUDC-907 displays potent antitumor activity against human pancreatic adenocarcinoma in vitro and in vivo through inhibition of HDAC6 to downregulate c-Myc expression. *Acta Pharmacol Sin* 40: 677-688, 2019.
16. Pal S, Kozono D, Yang X, Fendler W, Fitts W, Ni J, Alberta JA, Zhao J, Liu KX, Bian J, *et al*: Dual HDAC and PI3K inhibition abrogates NF kappa B- and FOXM1-mediated DNA damage response to radiosensitize pediatric high-grade gliomas. *Cancer Res* 78: 4007-4021, 2018.
17. Younes A, Berdeja JG, Patel MR, Flinn I, Gerecitano JF, Neelapu SS, Kelly KR, Copeland AR, Akins A, Clancy MS, *et al*: Safety, tolerability, and preliminary activity of CUDC-907, a first-in-class, oral, dual inhibitor of HDAC and PI3K, in patients with relapsed or refractory lymphoma or multiple myeloma: An open-label, dose-escalation, phase 1 trial. *Lancet Oncol* 17: 622-631, 2016.
18. Oki Y, Kelly KR, Flinn I, Patel MR, Gharavi R, Ma A, Parker J, Hafeez A, Tuck D and Younes A: CUDC-907 in relapsed/refractory diffuse large B-cell lymphoma, including patients with MYC-alterations: Results from an expanded phase I trial. *Haematologica* 102: 1923-1930, 2017.
19. Livak KJ and Schmittgen TD: Analysis of relative gene expression data using real-time quantitative PCR and the 2(-Delta Delta C(T)) method. *Methods* 25: 402-408, 2001.
20. Li M, Sun C, Bu X, Que Y, Zhang L, Zhang Y, Zhang L, Lu S, Huang J, Zhu J, *et al*: ISL1 promoted tumorigenesis and EMT via Aurora kinase A-induced activation of PI3K/AKT signaling pathway in neuroblastoma. *Cell Death Dis* 12: 620, 2021.
21. Hickman DL: Minimal exposure times for irreversible euthanasia with carbon dioxide in mice and rats. *J Am Assoc Lab Anim Sci* 61: 283-286, 2022.
22. Matthay KK, Maris JM, Schleiermacher G, Nakagawara A, Mackall CL, Diller L and Weiss WA: Neuroblastoma. *Nat Rev Dis Primers* 2: 16078, 2016.
23. Eleveld TF, Oldridge DA, Bernard V, Koster J, Colmet DL, Diskin SJ, Schild L, Bentahar NB, Bellini A, Chicard M, *et al*: Relapsed neuroblastomas show frequent RAS-MAPK pathway mutations. *Nat Genet* 47: 864-871, 2015.
24. Mlakar V, Morel E, Mlakar SJ, Ansari M and Gumy-Pause F: A review of the biological and clinical implications of RAS-MAPK pathway alterations in neuroblastoma. *J Exp Clin Cancer Res* 40: 189, 2021.
25. Veschi V, Verona F and Thiele CJ: Cancer stem cells and neuroblastoma: Characteristics and therapeutic targeting options. *Front Endocrinol (Lausanne)* 10: 782, 2019.
26. Aravindan N, Somasundaram DB, Herman TS and Aravindan S: Significance of hematopoietic surface antigen CD34 in neuroblastoma prognosis and the genetic landscape of CD34-expressing neuroblastoma CSCs. *Cell Biol Toxicol* 37: 461-478, 2021.
27. Mehrzama M, Madjd Z, Kalantari E, Panahi M, Hendi A and Sharifatabrizi A: Expression of stem cell markers, CD133 and CD44, in pediatric solid tumors: a study using tissue microarray. *Fetal Pediatr Pathol* 32: 192-204, 2013.
28. Mesrati MH, Syafruddin SE, Mohtar MA and Syahir A: CD44: A multifunctional mediator of cancer progression. *Biomolecules* 11: 1850, 2021.
29. Gomez KE, Wu F, Keysar SB, Morton JJ, Miller B, Chimed TS, Le PN, Nieto C, Chowdhury FN, Tyagi A, *et al*: Cancer cell CD44 mediates macrophage/monocyte-driven regulation of head and neck cancer stem cells. *Cancer Res* 80: 4185-4198, 2020.
30. Hsiao YW, Chi JY, Li CF, Chen LY, Chen YT, Liang HY, Lo YC, Hong JY, Chuu CP, Hung LY, *et al*: Disruption of the pentraxin 3/CD44 interaction as an efficient therapy for triple-negative breast cancers. *Clin Transl Med* 12: e724, 2022.
31. Zafar A, Wang W, Liu G, Wang X, Xian W, McKeon F, Foster J, Zhou J and Zhang R: Molecular targeting therapies for neuroblastoma: Progress and challenges. *Med Res Rev* 41: 961-1021, 2021.
32. Westhoff MA, Karpel-Massler G, Brühl O, Enzenmüller S, La Ferla-Bruhl K, Siegelin MD, Nonnenmacher L and Debatin KM: A critical evaluation of PI3K inhibition in glioblastoma and neuroblastoma therapy. *Mol Cell Ther* 2: 32, 2014.
33. Li Z and Thiele CJ: Targeting Akt to increase the sensitivity of neuroblastoma to chemotherapy: Lessons learned from the brain-derived neurotrophic factor/TrkB signal transduction pathway. *Expert Opin Ther Targets* 11: 1611-1621, 2007.
34. Boller D, Schramm A, Doepfner KT, Shalaby T, von Bueren AO, Eggert A, Grotzer MA and Arcaro A: Targeting the phosphoinositide 3-kinase isoform p110delta impairs growth and survival in neuroblastoma cells. *Clin Cancer Res* 14: 1172-1181, 2008.
35. Iwamoto M, Friedman EJ, Sandhu P, Agrawal NG, Rubin EH and Wagner JA: Clinical pharmacology profile of vorinostat, a histone deacetylase inhibitor. *Cancer Chemother Pharmacol* 72: 493-508, 2013.
36. Zorzi AP, Bernstein M, Samson Y, Wall DA, Desai S, Nicksy D, Nancy W, Elizabeth E and Sylvain B: A phase I study of histone deacetylase inhibitor, pracinostat (SB939), in pediatric patients with refractory solid tumors: IND203 a trial of the NCIC IND pro-gram/C17 pediatric phase I consortium. *Pediatr Blood Cancer* 60: 1868-1874, 2013.
37. Yang J, Nie J, Ma X, Wei Y, Peng Y and Wei X: Targeting PI3K in cancer: Mechanisms and advances in clinical trials. *Mol Cancer* 18: 26, 2019.
38. Chilamakuri R and Agarwal S: Dual targeting of PI3K and HDAC by CUDC-907 inhibits pediatric neuroblastoma growth. *Cancers (Basel)* 14: 1067, 2022.
39. Mondello P, Derenzini E, Asgari Z, Philip J, Brea EJ, Seshan V, Hendrickson RC, de Stanchina E, Scheinberg DA and Younes A: Dual inhibition of histone deacetylases and phosphoinositide 3-kinase enhances therapeutic activity against B cell lymphoma. *Oncotarget* 8: 14017-14028, 2017.
40. Vega FM, Colmenero-Repiso A, Gomez-Munoz MA, Rodriguez-Prieto I, Aguilar-Morante D, Ramirez G, Marquez C, Cabello R and Pardal R: CD44-high neural crest stem-like cells are associated with tumour aggressiveness and poor survival in neuroblastoma tumours. *EBioMedicine* 49: 82-95, 2019.
41. Fabian J, Lodrini M, Oehme I, Schier MC, Thole TM, Hielscher T, Kopp-Schneider A, Opitz L, Capper D, von Deimling A, *et al*: GRHL1 acts as tumor suppressor in neuroblastoma and is negatively regulated by MYCN and HDAC3. *Cancer Res* 74: 2604-2616, 2014.
42. Fabian J, Opitz D, Althoff K, Lodrini M, Hero B, Volland R, Beckers A, de Preter K, Decock A, Patil N, *et al*: MYCN and HDAC5 transcriptionally repress CD9 to trigger invasion and metastasis in neuroblastoma. *Oncotarget* 7: 66344-66359, 2016.

43. Chesler L, Schlieve C, Goldenberg DD, Kenney A, Kim G, McMillan A, Matthey KK, Rowitch D and Weiss WA: Inhibition of phosphatidylinositol 3-kinase destabilizes Mycn protein and blocks malignant progression in neuroblastoma. *Cancer Res* 66: 8139-8146, 2006.
44. Smith JR, Moreno L, Heaton SP, Chesler L, Pearson AD and Garrett MD: Novel pharmacodynamic biomarkers for MYCN protein and PI3K/AKT/mTOR pathway signaling in children with neuroblastoma. *Mol Oncol* 10: 538-552, 2016.
45. Valencia-Sama I, Ladumor Y, Kee L, Adderley T, Christopher G, Robinson CM, Kano Y, Ohh M and Irwin MS: NRAS status determines sensitivity to SHP2 inhibitor combination therapies targeting the RAS-MAPK pathway in neuroblastoma. *Cancer Res* 80: 3413-3423, 2020.
46. Chakrabarti L, Abou-Antoun T, Vukmanovic S and Sandler AD: Reversible adaptive plasticity: A mechanism for neuroblastoma cell heterogeneity and chemo-resistance. *Front Oncol* 2: 82, 2012.
47. Nassar D and Blanpain C: Cancer stem cells: Basic concepts and therapeutic implications. *Annu Rev Pathol* 11: 47-76, 2016.
48. Ross RA, Walton JD, Han D, Guo HF and Cheung NK: A distinct gene expression signature characterizes human neuroblastoma cancer stem cells. *Stem Cell Res* 15: 419-426, 2015.
49. Dong W, Xu X, Luo Y, Yang C, He Y, Dong X and Wang J: PTX3 promotes osteogenic differentiation by triggering HA/CD44/FAK/AKT positive feedback loop in an inflammatory environment. *Bone* 154: 116231, 2022.
50. Zhang H, Brown RL, Wei Y, Zhao P, Liu S, Liu X, Deng Y, Hu X, Zhang J, Gao XD, *et al*: CD44 splice isoform switching determines breast cancer stem cell state. *Genes Dev* 33: 166-179, 2019.
51. Louhichi T, Ziadi S, Saad H, Dhiab MB, Mestiri S and Trimeche M: Clinicopathological significance of cancer stem cell markers CD44 and ALDH1 expression in breast cancer. *Breast Cancer* 25: 698-705, 2018.
52. Elkashty OA, Elghanam GA, Su X, Liu Y, Chauvin PJ and Tran SD: Cancer stem cells enrichment with surface markers CD271 and CD44 in human head and neck squamous cell carcinomas. *Carcinogenesis* 41: 458-466, 2020.
53. Chen F, Chen X, Ren Y, Weng G, Keng PC, Chen Y and Lee SO: Radiation-induced glucocorticoid receptor promotes CD44+ prostate cancer stem cell growth through activation of SGK1-Wnt/beta-catenin signaling. *J Mol Med (Berl)* 97: 1169-1182, 2019.
54. Tomizawa F, Jang MK, Mashima T and Seimiya H: c-KIT regulates stability of cancer stemness in CD44-positive colorectal cancer cells. *Biochem Biophys Res Commun* 527: 1014-1020, 2020.
55. Sadeghi A, Roudi R, Mirzaei A, Zare MA, Madjd Z and Abolhasani M: CD44 epithelial isoform inversely associates with invasive characteristics of colorectal cancer. *Biomark Med* 13: 419-426, 2019.
56. Kumazoe M, Takai M, Bae J, Hiroi S, Huang Y, Takamatsu K, Won Y, Yamashita M, Hidaka S, Yamashita S, *et al*: FOXO3 is essential for CD44 expression in pancreatic cancer cells. *Oncogene* 36: 2643-2654, 2017.
57. Cai HY, Yu B, Feng ZC, Qi X and Wei XJ: Clinical significance of CD44 expression in children with hepatoblastoma. *Genet Mol Res* 14: 13203-13207, 2015.
58. Ghanem MA, Van Steenbrugge GJ, Van Der Kwast TH, Sudaryo MK, Noordzij MA and Nijman RJ: Expression and prognostic value Of CD44 isoforms in nephroblastoma (Wilms tumor). *J Urol* 168: 681-686, 2002.
59. Amirghofran Z, Asiaee E and Kamazani FM: Soluble CD44 and CD44v6 and prognosis in children with B-cell acute lymphoblastic leukemia. *Asia Pac J Clin Oncol* 12: e375-e382, 2016.
60. Legras S, Gunthert U, Stauder R, Curt F, Oliferenko S, Kluin-Nelemans HC, Marie JP, Proctor S, Jasmin C and Smadja-Joffe F: A strong expression of CD44-6v correlates with shorter survival of patients with acute myeloid leukemia. *Blood* 91: 3401-3413, 1998.



Copyright © 2023 Li et al. This work is licensed under a Creative Commons Attribution-NonCommercial-NoDerivatives 4.0 International (CC BY-NC-ND 4.0) License.